ACS APPLIED MATERIALS & INTERFACES

Research Article

www.acsami.org

Probing the Sensory Property of Perylenediimide Derivatives in Hydrazine Gas: Core-Substituted Aromatic Group Effect

Yongwei Huang,*[,†] Weiguang Zhang,[†] Junchao Wang,[†,‡] and Zhixiang Wei*[,‡]

[†]Institute of Molecular Medicine, Medical College, Henan University, Kaifeng 475004, China

[‡]National Center for Nanoscience and Technology, Beijing 100190, China

Supporting Information

ABSTRACT: In this contribution, four perylenediimide derivatives (PTCDIs) with different core-substituted aromatic groups were prepared. Studies on their sensing properties in hydrazine vapor (10 ppm) suggested ~5 orders of the magnitude in increased current for core-phenyl-substituted DEY was achieved and this value is 9, 9, and 24 times higher than that of core-pyridyl-substituted DSPY, DFPY, and DTPY, respectively. The differential response to the hydrazine vapor is less dependent on their surface area and morphologies. The lower LUMO energy and activation energy with smaller interplanar spacing allows DEY highly efficient sensing performance. A similar face−face packing mode and LUMO energy of DSPY and DFPY lead to both of them exhibiting the same sensing performance, while higher LUMO energy and head-to-tail packing modes with a greater interplanar spacing induce the less-efficient sensing performance of DTPY sensors. Discussions for structure−function relationships suggested that aromatic groups in the bay region have significant impact on PTCDI sensing performance by modulating energy level, interplanar spacing, and stacking modes.

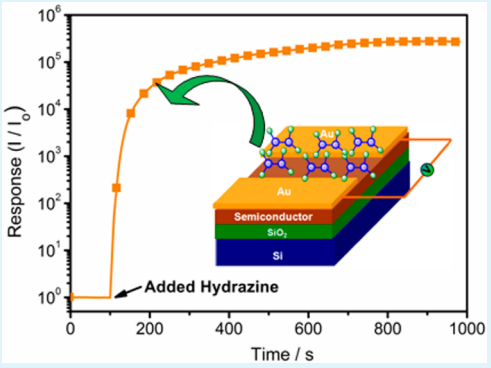

KEYWORDS: *perylenediimide derivatives, micro/nanostructure, sensory properties, response, core-substituted groups*

INTRODUCTION

Perylene and its derivatives are among the most extensively investigated chromospheres in dye chemistry, because of their high absorption coefficient for visible light as well as their high chemical and thermal stability.[1] They have found many potential applications in the materials[2−4] and supramolecular chemistry area.[5,6] Another possible application of perylenediimide derivatives (PTCDIs) is their use as gas-sensing devices,[7] which are based on a change in its fluorescence[8] or conductivity[9] under the influence of gas molecules. Recently, several groups have initiated programs to design gas fluorescent or conductometric sensing devices based on PTCDI molecules for detecting volatile organic vapor. Che et al. fabricated a sensing device based on microfibers fabricated of hexylheptyl-substituted PTCDIs, which has a high sensitivity to organic amines.[10] Liu and co-workers developed a new cyclodextrin-substituted PTCDI sensors with desired selectivity.[11] Peng et al. have used cholesterol-derived PTCDIs as materials, successfully creating amine-sensing devices with a detect limitation of 150.0 ppt.[12] To study the diffusion effect using electrical measurement methods, dimethylperylene-substituted PTCDIs conductometric sensing devices were prepared by Schlettwein's group, and changes in the conductivity were shown under increasing partial pressure of ethanol, acetone, or *n*-butane.[13] Although much success has been achieved for detection of volatile organic vapor by using PTCDI sensing devices,[14] the design and application of the PTCDIs sensing material lack a systematic nature, and the relationships between the molecular structure of PTCDIs and its sensing performance still remain veiled.

Variation in the electrical conductivity of organic semiconductor induced by the adsorption of gases represents one of the critical parameters to control the performance of conductometric gas sensors. In general, variance of conductivity is associated with chemical nature of organic semiconductor materials,[15] which is closely related to the molecular structure. Therefore, molecular modification is one of the most important means to improve the performance of PTCDI devices.[16] To date, most modifications of perylenediimide derivatives were achieved by introducing solubilizing substituted groups at the imide nitrogen or adding substituents to the carbocyclic scaffold in the so-called bay area.[17] Through latter strategy, some core substituents can be introduced to the conjugated core, which not only change energy level, but also lead to twisting of perylene core and alter $\pi-\pi$ overlap between naphthalenic subunits, to significantly affect the performance of PTCDIs devices.[18] Since the performance was associated with core-substituted groups, it is inferred that some valuable information about structure−function relationships can be revealed by

Received: March 20, 2014
Accepted: June 4, 2014
Published: June 4, 2014

   dx.doi.org/10.1021/am5016765 | ACS Appl. Mater. Interfaces 2014, 6, 9307−9313

detailed probing the effect of core-substituted groups on the performance of PTCDI conductometric sensors.

In the present study, four core-aromatic substituted perylenediimide derivatives: *N*′-bis(*n*-dodecyl)-1,7-di(phenylethynyl)perylene-3,4:9,10-tetracarboxyldiimide (DEY), *N*,*N*′-bis(*n*-dodecyl)-1,7-di(2-ethynylpyridine)perylene-3,4:9,10-tetracarboxyldiimide (DSPY), *N*,*N*′-bis(*n*-dodecyl)-1,7-di(3-ethynylpyridine)perylene-3,4:9,10-tetracarboxyldiimide (DTPY), *N*,*N*′-bis(*n*-dodecyl)-1,7-di(4-ethynylpyridine)-perylene-3,4:9,10-tetracarboxyldiimide (DFPY) (Scheme 1)

Scheme 1. Molecular Structure of DEY, DSPY, DTPY, and DFPY

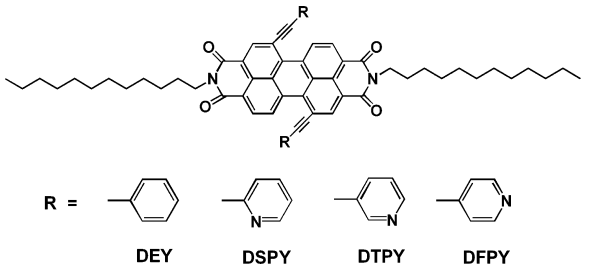

were prepared and their gas response to hydrazine vapor was characterized by conductivity measurements. This work mainly focuses on the effect of two types of aromatic groups—namely, phenyl and pyridyl—and isomeric effect of nitrogen atom in pyridyl ring on sensing performance of PTCDIs sensors. It was found that variation of aromatic groups and substituted position of nitrogen atom in pyridyl ring not only change energy level, but also lead to twisting of perylene core and remarkably affect solid-state aggregation modes so as to have significant impact on their gas responses. Detailed analyses of the effect of these core-substituted groups on sensing performance are presented.

EXPERIMENTAL SECTION

The synthesis and purification of DEY, DSPY, DTPY, and DFPY were synthesized according to reported procedure with slight modifications,[19] and the synthesis procedures was shown in the Supporting Information.^{1}H NMR spectra (400 MHz) were recorded on a Bruker ARX 400 with $CDCl_3$ or CF_3COOD as the solvent. The surface morphologies of spin-coated thin film on SiO_2/Si substrates were observed on a Nanoscope IIIa atomic force microscopy (AFM) system in tapping mode. Fluorescence spectra and ultraviolet−visible light (UV-vis) absorption spectra were recorded on a Perkin−Elmer Model LS 55 luminescence spectrometer and a Perkin−Elmer Model Lamda 950 UV−vis spectrophotometer, respectively. The X-ray diffraction (XRD) patterns of these PTCDI films were performed on a Model D/max-2500 rotation anode X-ray diffractometer (Rigaku, Japan), for which a Cu Kα radiation (λ = 1.54 Å) was used. Cyclic voltammetry was recorded on IM6ex under Ar in dichloromethane solutions with Ag/AgCl as the reference electrode. The film thickness was examined by Kla-Ten Alpha-step D-120 stylus profiler. The valence band (E_v) and the conduction band (E_c) was calculated according to corresponding highest occupied molecular orbital (HOMO) and lowest unoccupied molecular orbital (LUMO) energies. The LUMO energies for these PTCDIs were estimated, versus the vacuum level, according to E_{LUMO} = 4.4 eV − E_{red1}, and HOMO energies were obtained using the relation $E_{HOMO} = E_{LUMO} - E_g$ from the optical gaps (E_g) determined from the overlap of the normalized UV-vis and fluorescence spectra in dichloromethane (see Figure S1 in the Supporting Information). The Fermi level (E_F) was estimated from the average value of E_c and E_v.

DEY, DSPY, DTPY, and DFPY sensors were fabricated according to a procedure below. First, SiO_2-coated Si(100) substrates were cleaned in a 3:7 mixture of H_2O_2 and H_2SO_4, rinsed with deionized water, and dried by a stream of argon. Then, the chloroform solutions (2 mg mL^{-1}) of DEY, DSPY, DTPY, and DFPY were spin-coated on the substrates in air at room temperature. Finally, drain and source electrodes for current (I)−time (t) measurement were fabricated by vapor depositing Au (2×10^{-6} Torr, 0.5 Å/s, ∼50 nm thick) onto semiconductor film (80 nm) through shadow mask to obtain devices with a channel length of 100 μm and width of 110 μm. The device was put into the test chamber with a volume of 2 L, which was connected with vacuum with two-way valves. Then, a certain amount of hydrazine was injected into the test chamber by a syringe and the variation in current was recorded continuously by a Keithley Model 4200-SCS system until the current reached a steady value.

RESULTS AND DISCUSSION

As *n*-type organic semiconductor materials (i.e., electron acceptor), PTCDIs are capable of acting as sensory materials, which are used to examine some reducing agents (i.e., electron donor) such as hydrazine.[20] Therefore, the sensory properties of DEY, DSPY, DTPY, and DFPY films in hydrazine gas were investigated by their conductometric gas sensors, and the results revealed that these PTCDIs materials were highly sensitive to hydrazine vapor. To evaluate their sensing performance, the normalized current change I/I_0, where I and I_0 denote the real-time and the initial current, respectively, were recorded in Figure 1. Upon their exposure to hydrazine vapor

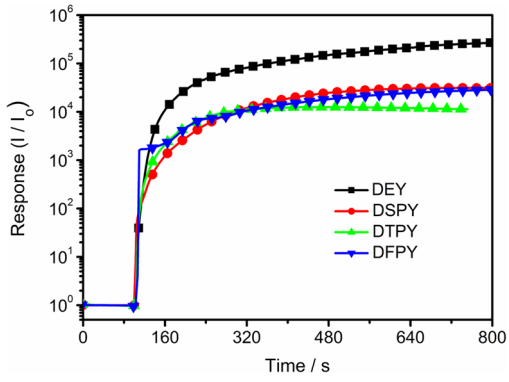

Figure 1. Current modulation (I/I_0)−time (t) curves of DEY, DSPY, DTPY, and DFPY gas sensors in hydrazine vapor (10 ppm).

(10 ppm), it was determined that an ∼5-orders-of-magnitude increase in current for DEY was achieved (Figure 1). Although a notable change was also observed in the current of DSPY, DTPY, and DFPY, the magnitude of increased current, compared with DEY, is 9, 9, and 24 times lower for DSPY, DFPY, and DTPY, respectively (see Figure 1). Some experiments, under changing concentration of hydrazine (Figure S2 in the Supporting Information) or the thickness of the PTCDI films (Figure S3 in the Supporting Information) were carried out further, and similar results can be achieved.

dx.doi.org/10.1021/am5016765 | ACS Appl. Mater. Interfaces 2014, 6, 9307−9313

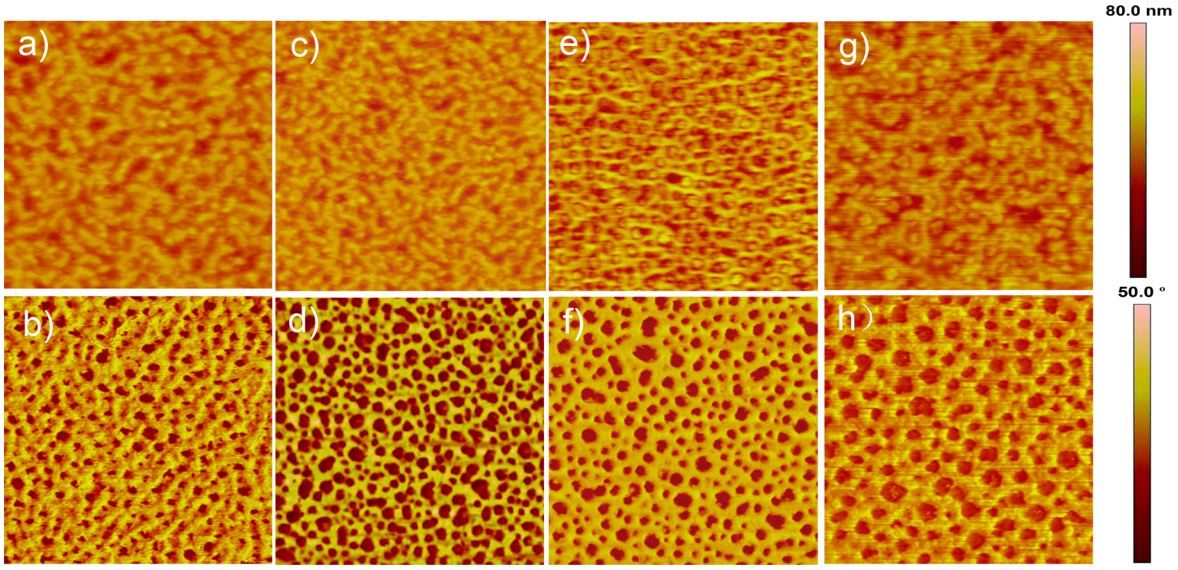

Figure 2. AFM images (5 μm × 5 μm) of thin films of (a, b) DEY, (c, d) DSPY, (e, f) DTPY and (g, h) DFPY. The upper row shows topographic images, and the lower row shows phase contrast images.

These results revealed core-phenyl substituted DEY molecules, which were more sensitive to hydrazine gas than core-pyridyl substituted DSPY, DTPY, and DFPY. Concerning pyridyl-substituted PTCDIs, DSPY and DFPY possess the same variations in the magnitude of current (~4 orders of magnitude) and the value is ~3 times higher than that of DTPY, which illustrate that the substituted position of the N atom also had a significant impact on the sensing performance of PTCDI gas sensors. Further compared with core-unsubstituted PTCDI-C_{12} and PTCDI-C_{10} (Table S1 in the Supporting Information),[14,21] the magnitude of increased current for core-aromatic-substituted DEY, DSPY, DFPY, and DTPY was 1−2 orders higher than that of PTCDI-C_{12} and PTCDI-C_{10}. This behavior can be ascribed to their larger delocalization of the perylene anionic radical and smaller activation energy.[22]

In general, the mechanism of conductometric gas sensors based on organic semiconductor materials is founded on the gas adsorption/binding at the surface, then formed charge transfer complexes between both species that dissociate and diffuse into the materials, which lead to the variation in the majority charge carriers, and then in the conductivity.[23] This mechanism can involve either weak or chemical interactions, depending on the chemical nature of both the gas and organic semiconductor materials. From the mechanism, it can be seen that the response or sensitivity of organic semiconductor materials is related to two factors. One is the high surface area that can provide the expedient diffusion of the analyte molecule, the other is the chemical or aggregated nature of semiconductor molecules such as energy level and molecular packing modes, which are associated with the formation of charge carriers and efficient transport into the materials. According to this sensing mechanism, the surface morphologies of the fabricated thin films were first investigated by AFM. As shown in Figure 2, although all films possess a similar morphology and exhibit a meshlike surface microstructure, a smaller magnitude of holes obviously exhibited in the film of DEY compared to DSPY, DTPY, and DFPY, which indicated the smallest surface area was contacted with the analyte. In the case of DSPY, DTPY, and DFPY, more ordered and dense holes were displayed in the thin film of DTPY, which provide high-efficient channel for diffusion of gas molecules. While a bigger holelike microstructure was found in the DFPY film, implying a smaller outside surface area and a less contact time with hydrazine vapor, and led to an abrupt increase in current (see Figure 1).[24] However, the DEY and DTPY possess the best and worst sensing performances, respectively, despite their smallest and largest surface area. Therefore, it is proposed that the dramatic difference in sensing performance was less dependent on their morphologies and surface area.

In order to reveal the reason for the dramatic difference in their sensing performance, the crystal phases of DEY, DSPY, DTPY, and DFPY thin films were further investigated by XRD measurement and highly crystalline structure was observed (Figure 3). XRD profiles indicate the long axis of the unit cell as

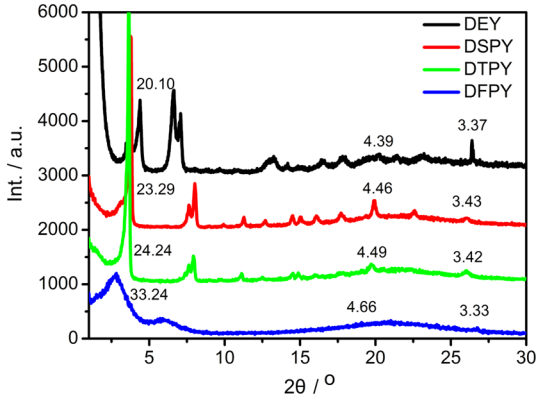

Figure 3. X-ray diffraction (XRD) patterns with *d* spacing given (Å) of DEY, DSPY, DTPY, and DFPY thin films.

20.10, 23.29, 24.24, and 33.24 Å (2θ = 4.39°, 3.79°, 3.64°, and 2.77°, respectively) for DEY, DSPY, DTPY, and DFPY, respectively, which is shorter than the total length of the corresponding PTCDI molecules of 40.46, 40.55, 40.32, and 40.73 Å (along the long axis of PTCDIs, DFT calculation, B3LYP/6-31g*). This is likely due to the tilted stacking of perylene core planes and the strong hydrophobic interaction

dx.doi.org/10.1021/am5016765 | ACS Appl. Mater. Interfaces 2014, 6, 9307−9313

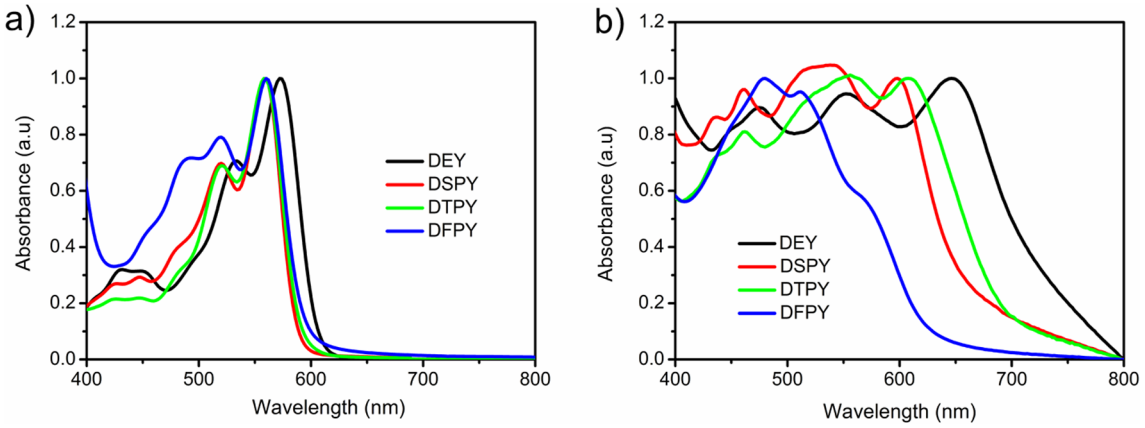

Figure 4. Normalized UV−vis spectra of DEY, DSPY, DTPY, and DFPY (a) in chloroform solution and (b) in films.

between side chains, which usually results in effective side-chain interdigitation and thus leads to shortened length along the longitudinal direction.[25] This result is further supported by a diffuse halo exhibiting in the wide-angle region (~20°, 4−5 Å), and this is attributed to the typical scattering from disordered alkyl chains, indicating that strong interdigitation between side chains. More importantly, a reflection was observed in the wide angle region at ca. 2θ = 26.44°, 25.98°, 26.02°, and 26.77° (interplanar spacings of 3.37, 3.43, 3.42, and 3.33 Å, respectively) for DEY, DSPY, DTPY, and DFPY, respectively, implying that strong $\pi-\pi$ stacking exists in the sample.[26] Since interplanar spacing between perylene core are crucial for efficient carrier transport, it can be speculated that variation in $\pi-\pi$ stacking distance may play an critical role in determining the sensing performance of PTCDIs.

UV-vis spectra were subsequently studied both in the chloroform and in thin films. As shown in Figure 4a, The UV-vis spectra of DEY, DSPY, DTPY, and DFPY in chloroform (0.1 mg mL^{-1}) exhibited three pronounced peaks (in the range of 450−620 nm) and a shoulder at ~430 nm. This is a typical spectrum of an individual PTCDI molecule in solution (i.e., in a nonaggregated form), and corresponds to an electronic $\pi-\pi^*$ transition superimposed with vibrational transitions.[27] In addition, the line shape of the absorption spectra for these core-substituted PTCDIs comparable to the spectra of unsubstituted one are broader and display less vibronic structures,[21] the difference can be explained in terms of the loss of planarity of the perylene core and the lower molecular symmetry caused by the bay substituents,[28] and this is supported by the results of calculated torsional angle, as discussed below. The solid-state spectra of the DEY, DSPY, DTPY, and DFPY thin films in air (Figure 4b) are significantly different from that in solutions. Compared to the spectra in solution, a dramatic red-shift of 74 nm for DEY, 15 nm for DTPY occurred in the spectra of thin films. This shift is due to the dipole-allowed low-energy absorption that is characteristic for transition dipoles in a head-to-tail configuration in a J-type aggregate.[29] In comparison, a remarkable blue-shift of 28 and 83 nm for DSPY and DFPY, respectively, exhibited in the spectra of thin films, implying the face−face parallel arrangement of chromophore dipoles in so-called H-aggregates.[30] Compared with J-type aggregate, H-aggregated mode implies more larger $\pi-\pi$ overlap of vicinal perylene core, which is expected to enhance charge carrier mobility.

In order to probe in-depth understanding for this dramatic difference in sensing performance, the torsional angles between the two naphthalene mean-square planes of perylene core were investigated using DFT/B3LYP program and the result is illustrated in Table 1. The results suggested that DEY possess the largest torsional angle of 17.29° in these PTCDIs. In the case of core-pyridyl substituted DSPY, DTPY, and DFPY, the torsional angle of 14.87° for DSPY, 16.99° for DTPY, and 17.03° for DFPY were found, indicating substituted position of the N atom also had significant impact on the torsion of perylene core. Combined with discussions on the XRD pattern, it is proposed that DEY an DTPY adopted a head-to-tail packing modes with a interplanar spacing of 3.37 and 3.45 Å, while DSPY and DFPY have a face-to-face molecular packing with contacts of 3.42 and 3.37 Å between the PTCDI π-planes (Figure 5), respectively. It is well-known that charge carrier mobility is usually maximized along the direction of cofacial

Table 1. Torsional Angles between the Two Naphthalene Mean-Square Planes of Perylene Core

semiconductor	torsional angle (deg)
DEY	17.29
DSPY	14.87
DTPY	16.99
DFPY	17.03

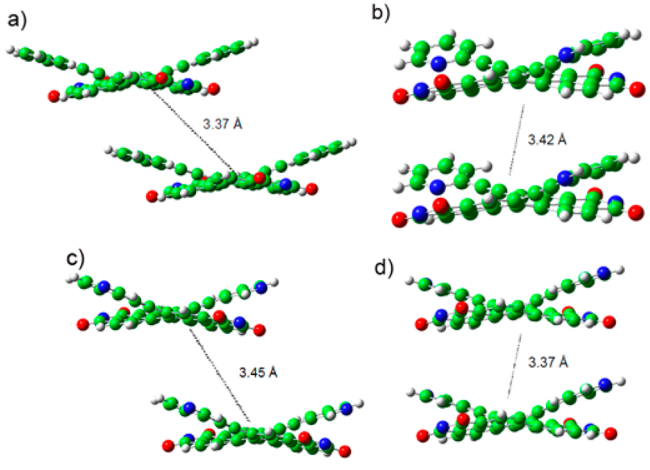

Figure 5. Possible packing styles of perylene core for (a) DEY, (b) DSPY, (c) DTPY, and (d) DFPY. These packing styles were obtained by analyzing DFT calculation results, UV-vis spectra, and XRD data.

dx.doi.org/10.1021/am5016765 | ACS Appl. Mater. Interfaces 2014, 6, 9307−9313

$\pi-\pi$ stacking of conjugated systems,[31] and thus the larger torsional angle must weaken the $\pi-\pi$ orbital overlap between adjacent perylene cores and depress carrier mobility and lead to a smaller magnitude of increase in current.

As far as an organic semiconductor is concerned, the electrical conductivity obeys the well-known Arrhenius-type equation that is described by eq 1:[32]

$$\sigma = \sigma_0 \exp(-E_a/kT) \quad (1)$$

where σ and σ_0 are the electrical conductivity and a prefactor, respectively, and E_a is the activation energy, k is the Boltzmann constant, and T is the temperature. E_a is given by either $E_c - E_F$ or $E_F - E_v$, depending on whether electrons or holes are considered. In the case of DEY, DSPY, DTPY, and DFPY molecules, the parameters σ_0, k, and T are same; therefore, the change of the electrical conductivity is only associated with the variation of E_a, which can be calculated from $E_c - E_F$, because only electron transport is occurring in these PTCDI solid materials. Therefore, we further investigated the electronic properties of all the present semiconductors via cyclic voltammetry (Figure 6), and the values of half-wave potentials

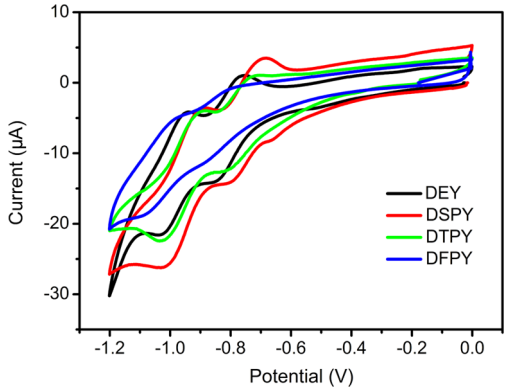

Figure 6. Cyclic voltammograms of reduction potentials for DEY, DSPY, DTPY, and DFPY in dichloromethane-TBAPF$_6$ (scan speed = 100 mV s^{-1}).

for the reduction (E_{red1}), LUMO, HOMO, E_c, E_v, E_F, and the corresponding E_a are summarized in Table 2. It was found that DEY possesses the lowest LUMO energy (−3.68 eV) and activation energy (2.10 eV) (see Table 2) among these PTCDI molecules. The lower LUMO energy and activation energy enable the high efficient charge exchange that occurs between DEY and hydrazine molecules (E°_{ox} = +0.43 V, vs. SCE), while close contacts of 3.37 Å between the adjacent perylene cores allows a very dense arrangement of the molecules, leading to high charge carrier mobility. Meanwhile, this close distance can well make up for a deficiency for carriers transport that arising from the head-to-tail arrangement and distorted packing of perylene core, and resulted in the most dramatic increase in current.

Concerning the DSPY and DSPY gas devices, the same magnitude of increased current was exhibited in hydrazine vapor. The behavior can be attributed to the differences in their interplanar spacing and torsional angle. As discussed earlier, both DSPY and DSPY adopted a face-to-face packing mode in thin films, implying a larger $\pi-\pi$ overlap of vicinal PTCDIs molecules that provide high-efficient channel for carrier transport. However, a greater torsional angle (17.03°) makes DFPY molecule larger distortion and reduces $\pi-\pi$ overlap between perylene core that hinder charge transport, despite DFPY allows for close interplanar spacing of 3.37 Å. Compared with DFPY, the molecule of DSPY showing a greater interplanar spacing of 3.42 Å within each stack induce a low-efficient charge transport, despite its smaller torsional angle of 14.87°, and thereby lead to the same variation in increasing current. This result is very consistent with the calculated electrical conductivity from the equation discussed above that are rooted in the same activation energy (see Table 2). In the case of DTPY sensors, the poorest sensing performance can be ascribed to two factors. The first one is DTPY molecules exhibiting the highest LUMO energy (−3.78 eV), which results in the charge exchange occurring between DTPY and hydrazine molecules being less efficient. The other one is the DTPY molecules adopting head-to-tail packing modes in thin films, showing a greater torsional angle of 16.99°, possessing a greater interplanar spacing of 3.45 Å, making the $\pi-\pi$ overlap minimal, and depress carrier mobility, and ultimately induce the smallest increasing in current.

CONCLUSION

In conclusion, four perylenediimide derivatives were prepared: DEY, DSPY, DTPY, and DFPY. The determination of sensing properties in hydrazine vapor based on their conductometric gas sensors revealed that an ∼5-order-of magnitude increase in current for core-phenyl-substituted DEY was achieved. This value is 9, 9, and 24 times higher than that of core-pyridyl-substituted DSPY, DTPY, and DFPY, respectively. The differential response to the hydrazine vapor for these PTCDI gas sensors is less dependent on their surface area and morphologies, and should be ascribed to difference in energy level, interplanar spacing and stacking modes. The lower LUMO energy and activation energy with smaller interplanar spacing allows DEY to possess a highly efficient sensing performance. A similar face-to-face packing mode and LUMO energy of DSPY and DFPY lead to both of them exhibiting same sensing performance, despite the differences in torsional angle and interplanar spacing. While higher LUMO energy and head-to-tail aggregated modes with a greater interplanar spacing induce the less-efficient sensing performance of DTPY sensors. This study indicates different types of aromatic groups in the bay region have significant impact on the performance of PTCDI gas-sensing devices. It is expected this study on structure−function relationships can provide some valuable

Table 2. Molecular Orbital Energies of the Organic Semiconductors Studied in This Work Estimated from Cyclic Voltammetry and Optical Absorption

semiconductor	E_{red1}	LUMO	HOMO	E_C (eV)	E_v (eV)	E_F (eV)	E_a (eV)
DEY	−0.72	−3.68	−5.78	−3.68	−5.78	−4.73	1.05
DSPY	−0.70	−3.70	−5.87	−3.70	−5.87	−4.79	1.08
DTPY	−0.61	−3.79	−5.94	−3.78	−5.94	−4.87	1.07
DFPY	−0.69	−3.71	−5.88	−3.71	−5.88	−4.80	1.08

dx.doi.org/10.1021/am5016765 | ACS Appl. Mater. Interfaces 2014, 6, 9307−9313

information on the design and development of high-performance organic sensing devices.

■ ASSOCIATED CONTENT

Supporting Information

Detailed synthesis procedures for compounds, UV−vis and fluorescence spectra and gas sensing performance of DEY, DSPY, DTPY, and DFPY. This material is available free of charge via the Internet at http://pubs.acs.org.

■ AUTHOR INFORMATION

Corresponding Authors

*Fax/Tel.: (+) 86-371-23880585. E-mail address: hywei79@126.com (Y. Huang).

*Fax/Tel.: (+) 86-10-82545565. Fax: (+)86-10-62656765. E-mail address: weizx@nanoctr.cn (Z. Wei).

Notes

The authors declare no competing financial interest.

■ ACKNOWLEDGMENTS

The authors gratefully acknowledge the National Natural Science Foundation of China (Nos. 21202036, 91027031, and 21125420), the Ministry of Science and Technology of China (Nos. 2009CB930400, 2010DFB63530, and 2011CB932300), China Postdoctoral Science Foundation (No. 2013M530335), and Henan University for financial support.

■ REFERENCES

(1) Kozma, E.; Catellani, M. Perylene Diimides Based Materials for Organic Solar Cells. *Dyes Pigm.* **2013**, *98*, 160−179.

(2) Günes, S.; Neugebauer, H.; Sariciftci, N. S. Conjugated Polymer-Based Organic Solar Cells. *Chem. Rev.* **2007**, *107*, 1324−1338.

(3) Shivanna, R.; Shoaee, S.; Dimitrov, S.; Kandappa, S. K.; Rajaram, S.; Durrant, J. R.; Narayan, K. S. Charge Generation and Transport in Efficient Organic Bulk Heterojunction Solar Cells with a Perylene Acceptor. *Energy Environ. Sci.* **2014**, *7*, 435−441.

(4) Arulkashmir, A.; Jain, B.; John, J. C.; Roy, K.; Krishnamoorthy, K. Chemically Doped Perylene Diimide Lamellae Based Field Effect Transistor with Low Operating Voltage and High Charge Carrier Mobility. *Chem. Commun.* **2014**, *50*, 326−328.

(5) Li, Y.; Li, H.; Li, Y.; Liu, H.; Wang, S.; He, X.; Wang, N.; Zhu, D. Energy Transfer Switching in a Bistable Molecular Machine. *Org. Lett.* **2005**, *7*, 4835−4838.

(6) Li, Y.; Zheng, H.; Li, Y.; Wang, S.; Wu, Z.; Liu, P.; Gao, Z.; Liu, H.; Zhu, D. Photonic Logic Gates Based on Control of FRET by a Solvatochromic Perylene Bisimide. *J. Org. Chem.* **2007**, *72*, 2878−2885.

(7) Feng, X.; An, Y.; Yao, Z.; Li, C.; Shi, G. A Turn-on Fluorescent Sensor for Pyrophosphate Based on the Disassembly of Cu^{2+}-Mediated Perylene Diimide Aggregates. *ACS Appl. Mater. Interfaces* **2012**, *4*, 614−618.

(8) Jiang, B. P.; Guo, D. S.; Liu, Y. Self-Assembly of Amphiphilic Perylene−Cyclodextrin Conjugate and Vapor Sensing for Organic Amines. *J. Org. Chem.* **2010**, *75*, 7258−7264.

(9) Huang, Y.; Fu, L.; Zou, W.; Zhang, F.; Wei, Z. Ammonia Sensory Properties Based on Single-Crystalline Micro/Nanostructures of Perylenediimide Derivatives: Core-Substituted Effect. *J. Phys. Chem. C* **2011**, *115*, 10399−10404.

(10) Che, Y.; Yang, X.; Loser, S.; Zang, L. Expedient Vapor Probing of Organic Amines Using Fluorescent Nanofibers Fabricated From an n-Type Organic Semiconductor. *Nano Lett.* **2008**, *8*, 2219−2224.

(11) Liu, Y.; Wang, K. R.; Guo, D. S.; Jiang, B. P. Supramolecular Assembly of Perylene Bisimide with β-Cyclodextrin Grafts as a Solid-State Fluorescence Sensor for Vapor Detection. *Adv. Funct. Mater.* **2009**, *19*, 2230−2235.

(12) Peng, H.; Ding, L.; Liu, T.; Chen, X.; Li, L.; Yin, S.; Fang, Y. An Ultrasensitive Fluorescent Sensing Nanofilm for Organic Amines Based on Cholesterol-Modified Perylene Bisimide. *Chem.—Asian J.* **2012**, *7*, 1576−1582.

(13) Graaf, H.; Schlettwein, D. Influence of Gas Molecules on the Charge Carrier Mobility in Thin Ffilms of Semiconducting Perylene Tetracarboxylic Imides. *J. Appl. Phys.* **2006**, *100*, 126104.

(14) Huang, Y.; Wang, J.; Fu, L.; Kuang, W.; Shi, J. Effect of Core-Substituted Groups on Sensing Properties Based on Single Micro/nanorod of Perylenediimide Derivatives. *Sens. Actuators B* **2013**, *188*, 411−416.

(15) Bohrer, M. I.; Sharoni, A.; Colesniuc, C.; Park, J.; Schuller, I. K.; Kummel, A. C.; Trogler, W. C. Gas Sensing Mechanism in Chemiresistive Cobalt and Metal-Free Phthalocyanine Thin Films. *J. Am. Chem. Soc.* **2007**, *129*, 5640−5646.

(16) Huang, C.; Barlow, S.; Marder, S. R. Perylene-3,4,9,10-tetracarboxylic Acid Diimides: Synthesis, Physical Properties, and Use in Organic Electronics. *J. Org. Chem.* **2011**, *76*, 2386−2407.

(17) Würthner, F. Perylene-3,4,9,10-tetracarboxylic Acid Diimides: Synthesis, Physical Properties, and Use in Organic Electronics. *Chem. Commun.* **2004**, 1564−1579.

(18) Schmidt, R.; Oh, J. H.; Sun, Y. S.; Deppisch, M.; Krause, A. M.; Radacki, K.; Braunschweig, H.; Könemann, M.; Erk, P.; Bao, Z.; Würthner, F. High-Performance Air-Stable n-Channel Organic Thin Film Transistors Based on Halogenated Perylene Bisimide Semiconductors. *J. Am. Chem. Soc.* **2009**, *131*, 6215−6228.

(19) Nolde, F.; Pisula, W.; Müller, S.; Kohl, C.; Müllen, K. Synthesis and Self-Organization of Core-Extended Perylene Tetracarboxydiimides with Branched Alkyl Substituents. *Chem. Mater.* **2006**, *18*, 3715−3725.

(20) Zang, L.; Che, Y.; Moore, J. S. One-Dimensional Self-Assembly of Planar π-Conjugated Molecules: Adaptable Building Blocks for Organic Nanodevices. *Acc. Chem. Res.* **2008**, *41*, 1596−1608.

(21) Huang, Y.; Fu, L.; Zou, W.; Zhang, F. Probing the Effect of Substituted Groups on Sensory Properties Based on Single-Crystalline Micro/Nanostructures of Perylenediimide Dyes. *New. J. Chem.* **2012**, *36*, 1080−1084.

(22) This behavior can be ascribed to two factors. The first one was that core-aromatic substituted DEY, DSPY, DFPY and DTPY possess lower E_a of 1.05−1.08 eV (Table 2) that leaded to a larger magnitude in increased current according to the electrical conductivity equation shown in this paper. The second fact was the introduction of aromatic groups into bay area that benefited to the formation of a larger delocalized system between perylene unit and phenyl or pyridyl substitents.[14] When reacting with hydrazine, DEY, DSPY, DFPY and DTPY were reduced to an anionic radical, and this structure was stable due to larger delocalization of the anionic radical,[20] which would decrease the recombination of electron−hole pairs and made the high efficiency of carriers transport and thus leaded to improvement of current.[20]

(23) Muzikante, I.; Parra, V.; Dobulans, R.; Fonavs, E.; Latvels, J.; Bouvet, M. A Novel Gas Sensor Transducer Based on Phthalocyanine Heterojunction Devices. *Sensors* **2007**, *7*, 2984−2996.

(24) Huang, Y.; Quan, B.; Wei, Z.; Liu, G.; Sun, L. Self-assembled Organic Functional Nanotubes and Nanorods and Their Sensory Properties. *J. Phys. Chem. C* **2009**, *113*, 3929−3933.

(25) Balakrishnan, K.; Datar, A.; Naddo, T.; Huang, J.; Oitker, R.; Yen, M.; Zhao, J.; Zang, L. Effect of Side-Chain Substituents on Self-Assembly of Perylene Diimide Molecules: Morphology Control. *J. Am. Chem. Soc.* **2006**, *128*, 7390−7398.

(26) Chen, Z.; Stepanenko, V.; Dehm, V.; Prins, P. L.; Siebbeles, D. A.; Seibt, J.; Marquetand, P.; Engel, V.; Würthner, F. Photoluminescence and Conductivity of Self-Assembled π−π Stacks of Perylene Bisimide Dyes. *Chem.—Eur. J.* **2007**, *13*, 436−449.

(27) Jones, B. A.; Faccetti, A.; Wasielewski, M. R.; Marks, T. J. Tuning Orbital Energetics in Arylene Diimide Semiconductors. Materials Design for Ambient Stability of *n*-Type Charge Transport. *J. Am. Chem. Soc.* **2007**, *129*, 15259−15278.

(28) Chen, Z.; Baumeister, U.; Tschierske, C.; Würthner, F. Effect of Core Twisting on Self-Assembly and Optical Properties of Perylene Bisimide Dyes in Solution and Columnar Liquid Crystalline Phases. *Chem.—Eur. J.* **2007**, *13*, 450−465.
(29) Beckers, E. H. A.; Meskers, S. C. J.; Schenning, A. P. H. J.; Chen, Z.; Würthner, F.; Marsal, P.; Beljonne, D.; Cornil, J.; Janssen, R. A. J. Influence of Intermolecular Orientation on the Photoinduced Charge Transfer Kinetics in Self-Assembled Aggregates of Donor−Acceptor Arrays. *J. Am. Chem. Soc.* **2006**, *128*, 649−657.
(30) Ghosh, S.; Li, X. Q.; Stepanenko, V.; Würthner, F. Control of H- and J-Type π Stacking by Peripheral Alkyl Chains and Self-Sorting Phenomena in Perylene Bisimide Homo- and Heteroaggregates. *Chem.—Eur. J.* **2008**, *14*, 11343−11357.
(31) Hoeben, F. J. M.; Jonkheijm, P.; Meijer, E. W.; Schenning, A. P. H. J. About Supramolecular Assemblies of π-Conjugated Systems. *Chem. Rev.* **2005**, *105*, 1491−1546.
(32) Borker, A. D.; Gupta, M. C.; Umare, S. S. Electrical and Optical Properties of Conducting Copolymer: Poly(Aniline-Co-*n*-Ethylaniline). *Polym.-Plast. Technol. Eng.* **2001**, *40*, 225−234.